Biochemical Pharmacology, Vol. 56, pp. 1471–1479, 1998.

ISSN 0006-2952/98/$19.00 + 0.00
PII S0006-2952(98)00249-4

Interaction of the Antitumor Antibiotic Chromomycin A_3 with Glutathione, a Sulfhydryl Agent, and the Effect upon Its DNA Binding Properties

Sukanya Chakrabarti, Pulak Roy and Dipak Dasgupta†*
BIOPHYSICS DIVISION, SAHA INSTITUTE OF NUCLEAR PHYSICS, CALCUTTA-700 037, INDIA

ABSTRACT. Chromomycin A_3 (CHR), an anticancer antibiotic, blocks macromolecular synthesis via reversible interaction with DNA only in the presence of divalent cations like Mg^{2+}. In the absence of DNA, the antibiotic forms a dimer: Mg^{2+} complex [$(CHR)_2Mg^{2+}$]. It is the DNA-binding ligand. The antibiotic has potential reactive centers that could interact with GSH, the most abundant non-protein thiol in eukaryotic cells and a putative cofactor involved in the activation of many antibiotics *in vivo*. To understand the mode of action of CHR *in vivo*, we studied the interactions of CHR and the $(CHR)_2Mg^{2+}$ complex with GSH and the association of the resultant complexes with DNA by means of absorption, fluorescence, and circular dichroism spectroscopy. The novel finding was that GSH interacts non-covalently with CHR without a chemical modification of the antibiotic. The interaction was reversible in nature. The results are reported in two parts: the interaction of CHR with GSH in the absence and presence of Mg^{2+}, and the effect of this interaction on the DNA-binding properties of the antibiotic. CHR forms a single type of complex with GSH. In contrast, $(CHR)_2Mg^{2+}$ forms two different types of complexes with GSH: a low GSH complex at $\sim$ 12 mM GSH and a high GSH complex at $\geq$ 16 mM GSH. Binding and thermodynamic parameters for the reversible association of the complexes with DNA demonstrated that they bind differently to the same DNA. The thermodynamic parameters indicate that the presence of GSH alters the mode of binding of the $(CHR)_2Mg^{2+}$ complex with DNA. The $(CHR)_2Mg^{2+}$ complex binds to DNA via an entropy-driven process, whereas in the presence of GSH the association is enthalpy-driven. The significance of these results in the understanding of the molecular basis of action of the antibiotic is discussed. BIOCHEM PHARMACOL **56**;11:1471–1479, 1998. © 1998 Elsevier Science Inc.

KEY WORDS. anticancer antibiotic; chromomycin A_3; glutathione; DNA binding; chromomycin A_3 dimer–Mg^{2+} complex; absorbance, fluorescence and circular dichroism spectroscopy

CHR‡ (Fig. 1) is an antitumor antibiotic produced from *Streptomyces griseus* [1]. It reversibly binds to double-stranded DNA and blocks its function as a template for DNA and RNA polymerases [2]. Studies using optical and NMR spectroscopy [3, 4], and enzymatic and chemical foot printing [5, 6] demonstrated that the antibiotic binds via the minor groove with a GC base specificity. It was attributed to H-bonding between potential sites in the antibiotic, such as the OH group at C8 with the NH2 and N3 group of the guanine base [7]. The reversible interaction with DNA requires the presence of a divalent metal ion such as Mg^{2+}. We showed that in the absence of DNA the antibiotic forms two types of complexes with Mg^{2+}. These complexes are DNA-binding ligands [8]. The complexes, I (with 1:1 stoichiometry in terms of drug: Mg^{2+}) and II (with 2:1 stoichiometry in terms of drug: Mg^{2+}), bind differently to the same DNA, as indicated from the values of the binding stoichiometry and thermodynamic parameters [9, 10]. Complex II, i.e. $(CHR)_2Mg^{2+}$, is the plausible species formed at a millimolar level of intracellular Mg^{2+}.

Not much is known about the mode of action of the antibiotic *in vivo* except that it binds reversibly to DNA in the process of blocking its function as a template. The antibiotic has potential reactive centers such as the carbonyl group in the aglycone ring (see Fig. 1) for redox reactions with appropriate cytosolic components. Assessment of such interactions will be relevant in understanding the mode of action of the antibiotic *in vivo*, because the drug will encounter them during its transport to the nucleus. An important cytosolic component is GSH. GSH along with its oxidized form forms a very potent redox system ($E^{\circ} = -240$ mV) [11], which often detoxifies the

* Present address: Chemistry Department, Seth Anandram Jaipuria College, 10, Raja Naba Krishna St., Calcutta-700 005, India.
† Corresponding author: Dr. Dipak Dasgupta, Biophysics Division, Saha Institute of Nuclear Physics, 37, Belgachhia Road, Calcutta-700 037, India. Tel. (91)-(33)-556-5611; E-mail: dipak@biop.saha.ernet.in
‡ *Abbreviations:* A.U., arbitrary units; AUFS, absorbance unit full scale; CD, circular dichroism; CHR, chromomycin A_3; CT DNA, calf thymus DNA; and poly(dA-dT), double-stranded poly(dA-dT) · poly(dA-dT).
Received 11 February 1998; accepted 28 July 1998.

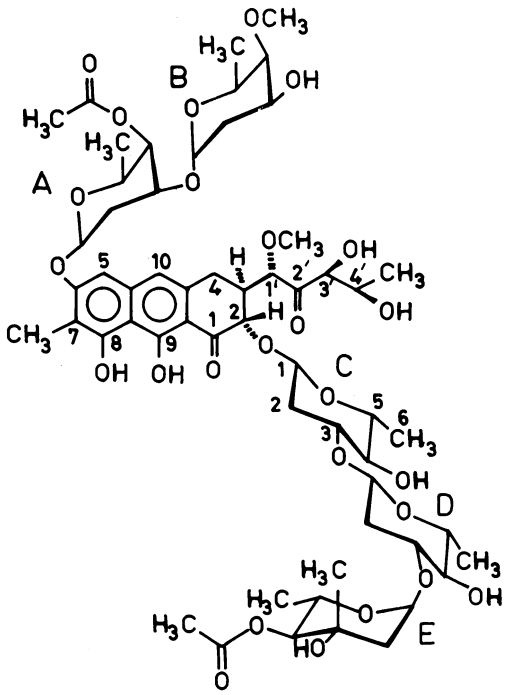

FIG. 1. Structure of chromomycin A_3.

cell via radical intermediate formation. These intermediates cause DNA damage and increase the cytotoxicity of the antibiotics. GSH is present at a relatively high concentration in the normal cell (0.5 to 10 mM) [12], the levels of which may go up further in the presence of carcinogens or in tumor cells [13, 14]. It interacts reductively with a number of antibiotics such as neocarzinostatin, calicheamicin, and bleomycin, generating active radical intermediates [15, 16]. On the other hand, the cytotoxicity of several covalently binding antibiotics like cisplatin, melphalan, and Adriamycin® is reduced considerably in the presence of GSH by its potential to scavenge free radicals inside the cell [17]. The presence of GSH in the cell also increases the radioresistance of the cell [18]. In view of these results, we have examined in this study the interaction of GSH with CHR under *in vitro* conditions. The effect of the binding of GSH upon the DNA-binding property of the antibiotic also has been followed because DNA is the major cellular target of the antibiotic. This part of the study had two objectives: (1) identifying any possible *in vivo* modification of the antibiotic by GSH, and (2) accounting for the high cytotoxicity of the antibiotic.

A significant result from the present studies was the finding that the antibiotic bound reversibly to GSH in the absence and presence of Mg^{2+}. There was no covalent modification of the antibiotic. This finding is novel and hitherto unreported for any other antibiotic. We have divided our results into two parts. The first part describes the interaction between CHR and the $(CHR)_2Mg^{2+}$ complex formed at a millimolar concentration of Mg^{2+} [8, 9] with GSH. The second part reports the DNA-binding properties of the GSH-bound $(CHR)_2Mg^{2+}$ complex. Thermodynamic parameters for DNA binding were determined for GSH-bound forms of $(CHR)_2Mg^{2+}$ to characterize the mode of binding.

All studies were carried out at pH 8.0 where a homogeneous population of negatively charged drug (pK_a 7.0) exists [19]. GSH is also negatively charged at this pH. CT DNA was chosen as the natural DNA model because it consists of comparable percentages of AT and GC base pairs.

MATERIALS AND METHODS

Chromomycin A_3, Tris, magnesium chloride solution (4.9 M), and CT DNA were from the Sigma Chemical Co. Poly(dA-dT), Sephacryl S-1000, and agarose were from Pharmacia Biotech Ltd. GSH, methanol, acetic acid, ammonium acetate, and sodium chloride were from the Sisco Research Laboratory. The purity of GSH was checked. Unless mentioned otherwise, studies were done in 20 mM Tris–HCl plus 100 mM NaCl buffer, pH 8.0. All buffers were prepared in deionized, all quartz distilled water. Absorption, fluorescence, and CD spectra were recorded with an Hitachi U-2000 spectrophotometer, a Shimadzu RF-540 spectrofluorometer, and a Jasco 720 spectropolarimeter, respectively. We determined the concentration of the antibiotic, DNA samples, and polynucleotides from their known molar extinction coefficients. The concentration of GSH, estimated by the enzymatic assay [20], was standardized against the dry weight of the chemical. GSH was stored under anhydrous conditions in the dark at a low temperature. A fresh solution of GSH was prepared as needed, just prior to use.

CT DNA was deproteinized by the chloroform-phenol extraction method and precipitated with ethanol. Then it was redissolved in 20 mM Tris–HCl buffer, pH 8.0, dialyzed extensively against the same buffer containing 5 mM EDTA to remove metal ions, and finally dialyzed against the buffer minus EDTA to remove EDTA.

The *pARC035* plasmid was isolated from its host strain, *JM101*, by alkali lysis method [21]. Final purification of the supercoiled plasmid DNA from RNA and relaxed plasmid DNA was done by Sephacryl S-1000 column chromatography. Purity of the circular DNA was checked by agarose gel electrophoresis.

Fluorescence measurements for the antibiotics and the $(CHR)_2Mg^{2+}$ complex in the presence and absence of GSH were carried out at an excitation wavelength of 470 nm instead of the absorption maximum at 405 nm, to avoid photodegradation [9]. Optical density of the samples at 470 nm did not exceed 0.02. Therefore, we did not correct the emission intensity for an optical filtering effect. Background emission (<5% of maximum) was corrected for by subtracting signals from blank buffer or GSH plus buffer samples. CD values are expressed as observed ellipticity (θ_{obs}) in millidegrees. CD spectra were measured in a 10-mm path-length cuvette as an average of two runs. They

were subtracted from buffer blank or GSH plus buffer samples, and smoothed within permissible limits by the inbuilt software of the instrument.

An LKB Superpac Cartridge column (4 × 125 mm), Spherisorb ODS2 (3 μm) was used for reversed-phase HPLC. The GSH complex was prepared by mixing 50 μM CHR with 16 mM GSH in 20 mM Tris–HCl plus 100 mM NaCl, pH 8.0, and incubated in the dark for 30 min. Fifty microliters of this sample was loaded into the column. The elution buffer was a gradient running from 100 to 0% methanol in the aqueous phase, 10 mM NH_4Ac/Ac buffer, pH 6.2. Eluted fractions were detected for CHR from fluorescence emission at 540 nm (λ_{ex} = 470 or 405 nm).

Supercoiled plasmid DNA was incubated with GSH-bound $(CHR)_2Mg^{2+}$ and run on a gel to detect any change in the DNA topology caused by ligand-induced relaxation or nicks [22]. The $(CHR)_2Mg^{2+}$ complex (formed by mixing 196.3 μM CHR with 20 mM $MgCl_2$ in the dark for 1 hr) was incubated separately with 12.3 and 18.0 mM GSH for 30 min in the dark at 25°, in 20 mM Tris–HCl, plus 100 mM NaCl, pH 8.0. Then GSH-bound complex was incubated with 193 μM plasmid DNA for a period of 4 hr, under the same conditions. The total sample volume of 12 μL was mixed with 2 μL of bromophenol blue dye and run on a 0.7% agarose gel. This was followed by ethidium bromide staining to detect any change in the migration of the complex-bound DNA with respect to the free DNA or DNA plus GSH, which were also loaded as controls.

Analysis of Binding Data

The binding isotherms were obtained by incubating the GSH plus $(CHR)_2Mg^{2+}$ complex with DNA in the buffer at different ratios of DNA and drug at a particular temperature, and monitoring the change in emission intensity at 540 nm (λ_{ex} = 470 nm) due to binding with the DNA. The spectrofluorometric titration data of the GSH-bound $(CHR)_2Mg^{2+}$ complexes with CT DNA were analyzed by two methods: curve fitting and Scatchard analysis.

In the model-independent curve-fitting method, the apparent binding constant was determined from the dissociation constant that fitted best to the experimentally obtained points. Here the ligand–DNA reaction was considered according to the following equilibrium: L + D = L-D. At a fixed concentration of the ligand and increasing concentrations of DNA, the titration profile shows the increase in the fluorescence intensity of the ligand as it binds to DNA. For an initial concentration "a" of the ligand and an input concentration "b" of DNA, the concentration of L-D is given by "x," such that the dissociation constant K_d takes the form, $K_d = (a - x) \cdot (b - x)/x$. Replacing "$x$" by the spectroscopic signal "S," the above equation takes the form:

$$K_d = [a - (\Delta S_{obs}/\Delta S_{max}) \cdot a] \cdot [b - \Delta S_{obs}/\Delta S_{max}) \cdot a]/ [(\Delta S_{obs}/\Delta S_{max}) \cdot a],$$

where $\Delta S_{obs} = (S_{obs} - S_0)$, $\Delta S_{max} = (S_{max} = S_0)$, and S_0 is the initial signal value of ligand when no DNA has been added. A program determines the value of K_d for each experimental value of b and ΔS_{obs}. ΔS_{max} was determined from the double-reciprocal plot [23]. Finally, a theoretical curve was constructed using the best fit value for K_d (= $1/K_{app}$).

The Scatchard plot is given by the equation $r/C_f = K_0 (n - r)$, where $r = C_b/C_p$ (C_b is the concentration of the bound ligand and C_p is the concentration of the DNA); n is the binding stoichiometry in terms of the number of drug molecules bound per nucleotide, and K_0 is the intrinsic binding constant. The apparent binding constant K_{app} is given by $K_0 \cdot n$. The dequenching of the fluorescence of the ligand as a function of added concentration of DNA was analyzed to construct the binding isotherm according to the Scatchard method. C_b was calculated as follows: $C_b = Q/Q_{max} \cdot C_{tot}$, where C_{tot} is the initial input concentration of the ligand, Q is the fractional dequenching during titration, and Q_{max} is the fractional dequenching when the ligand is totally bound to DNA [24]. Q is determined from the relation $Q = (I - I_0)/I_0$, where I_0 and I are the emission intensities of the free ligand and DNA bound ligand, respectively; $Q_{max} = (I_{max} - I_0)/I_0$, where I_{max} is obtained from a plot of $1/(I - I_0)$ against $1/(C_p - C_b)$, for which the intercept yields the value of $1/(I_{max} - I_0)$ [23]. This approach is based on the assumption of a linear relation between emission intensity and the concentration of the ligand, which was found to be valid for the concentration range of 5–50 μM of the ligand employed. The experimental points for the binding isotherm were subjected to least squares analysis with a view to getting a best-fit straight line.

The two methods were employed to analyze the binding data in order to check the internal consistency. This is particularly necessary when the affinity constant values are in the moderate range and the ligands are bulky.

The thermodynamic parameters ΔH (van't Hoff enthalpy), ΔS (entropy), and ΔG (free energy) were determined using the following equations: in $K_{app} = -\Delta H/RT + \Delta S/R$ and $\Delta G = \Delta H - T\Delta S$, where R and T are the universal gas constant and absolute temperature, respectively [25]. K_{app} was determined at four temperatures: 20°, 25°, 30°, and 35°, respectively, to evaluate ΔH and ΔS, and these values were incorporated in the equation to obtain the value of ΔG at room temperature.

RESULTS

Interaction of CHR and Its $(CHR)_2Mg^{2+}$ Complexes with GSH

Changes in the absorbance and CD spectrum showed that CHR and $(CHR)_2Mg^{2+}$ complex bound to GSH (Fig. 2 and 3). The absorption spectra for GSH-bound CHR and $(CHR)_2Mg^{2+}$ complex are shown in Fig. 2a and 3a, respectively. Common features for the change in the absorption spectra were broadening, a red shift of the peak, and hypochromicity when they were compared with the spectrum for

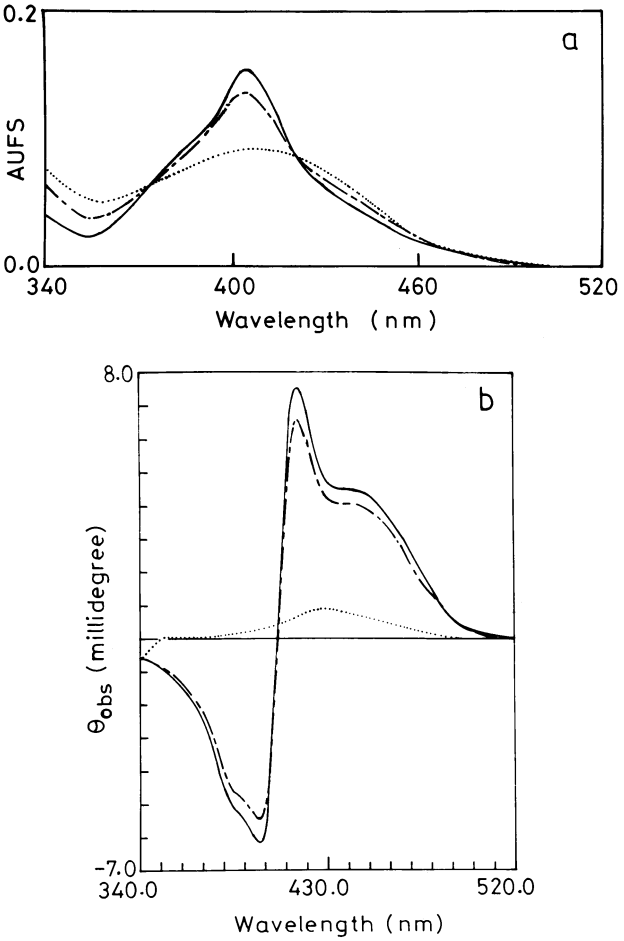

FIG. 2. (a) Absorption spectra of CHR under different conditions in 20 mM Tris–HCl plus 100 mM NaCl buffer, pH 8.0, at 25°: (1) CHR (15.0 μM) alone (———); and (2) CHR (15.0 μM) in the presence of GSH [10.3 mM (— · —) and 17.4 mM (· · · · · · · · ·)]. The reference cuvette contained the above buffer and GSH at the same concentration as in the sample cuvette. (b) CD spectra (340–520 nm) of CHR under different conditions in 20 mM Tris–HCl plus 100 mM NaCl buffer, pH 8.0, at 25°: (1) CHR (15.0 μM) alone (———); and (2) CHR (15.0 μM) in the presence of GSH [10.7 mM (— · —) and 16.0 mM (· · · · · · · · ·)].

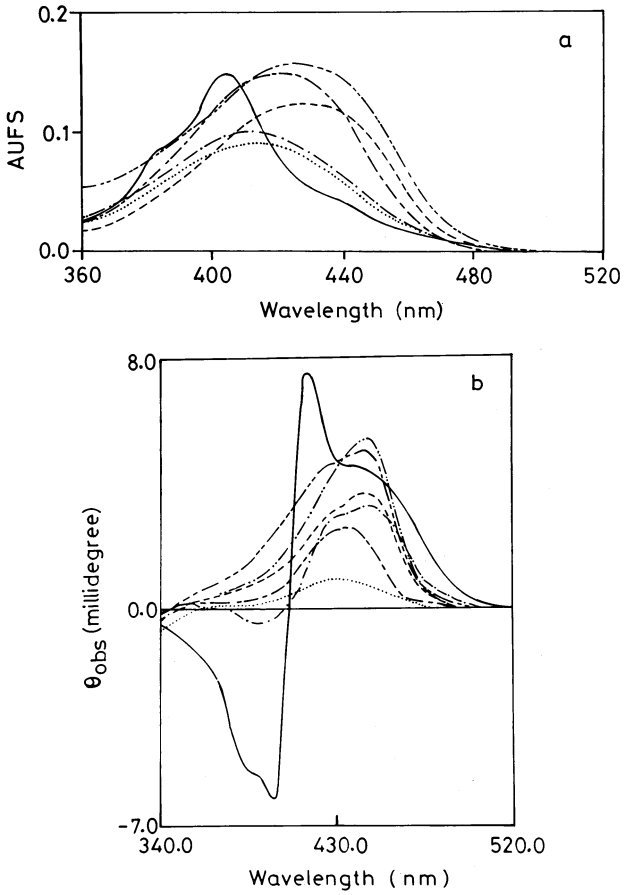

FIG. 3. (a) Absorption spectra of CHR, $(CHR)_2Mg^{2+}$ complex, and the low and the high complexes of GSH alone and in the presence of the different concentrations of CT DNA in 20 mM Tris–HCl plus 100 mM NaCl buffer, pH 8.0, at 25°: (1) CHR (15.7 μM) alone (———); (2) $(CHR)_2Mg^{2+}$ complex containing 15.7 μM CHR and 12.0 mM $MgCl_2$ (· — · —); (3) low GSH complex [$(CHR)_2Mg^{2+}$ complex plus GSH (12.0 mM, — · — · —)]; (4) low GSH complex in the presence of CT DNA (314 μM, – – – –); (5) high GSH complex [$(CHR)_2Mg^{2+}$ complex plus GSH (18.0 mM, · · · · · · · ·)]; and (6) high GSH complex in the presence of CT DNA (750 μM, – – — – – —). (b) CD spectra (340–520 nm) of CHR, $(CHR)_2Mg^{2+}$ complex, and the low and high GSH complexes alone and in the presence of different concentrations of CT DNA in 20 mM Tris–HCl plus 100 mM NaCl buffer, pH 8.0, at 25°. For comparison, the spectra for the $(CHR)_2Mg^{2+}$ complex in the presence of a saturating concentration of CT DNA is also given: (1) CHR (15.0 μM) alone (———); (2) $(CHR)_2Mg^{2+}$ complex containing 15.0 μM CHR and 12.0 mM $MgCl_2$ (– — – —); (3) low GSH complex [$(CHR)_2Mg^{2+}$ complex plus GSH (12.3 mM, — · —)]; (4) low GSH complex in the presence of CT DNA (330 μM, – – – –); (5) high GSH complex [$(CHR)_2Mg^{2+}$ complex plus GSH (18.9 mM, · · · · · · · ·)]; (6) high GSH complex in the presence of CT DNA (600 μM, – – — – – —); and (7) $(CHR)_2Mg^{2+}$ complex in the presence of CT DNA (220 μM, — · · —).

the free CHR. The spectrum of GSH-bound $(CHR)_2Mg^{2+}$ complex showed a blue shift with respect to that of free $(CHR)_2Mg^{2+}$complex. CD spectral change of CHR provided further evidence in favor of its association with GSH (Fig. 2b). There was a sharp decrease in the intensity of the CD bands when the input concentration of GSH changed from 10.7 to 16 mM. While the change in CD spectra indicated the interaction of $(CHR)_2Mg^{2+}$ complex with GSH, the nature of the change as a function of the input concentration of GSH was remarkably different from the previous example (Fig. 3b). The addition of GSH led to an initial increase in the ellipticity around 450 nm. It continued until ~12mM GSH, when the peak became relatively broad. At a higher GSH concentration (~18 mM), the ellipticity decreased with a concomitant broadening of the spectrum. It suggests that in the concentration range of 10 to 12 mM GSH, a different species is formed in the case of the $(CHR)_2Mg^{2+}$ complex. Absorption spectroscopy did not indicate the formation of such an intermediate complex. Illustrative titration profiles for the binding of $(CHR)_2Mg^{2+}$ complex to GSH using two different spectroscopic techniques are shown in Fig. 4. The

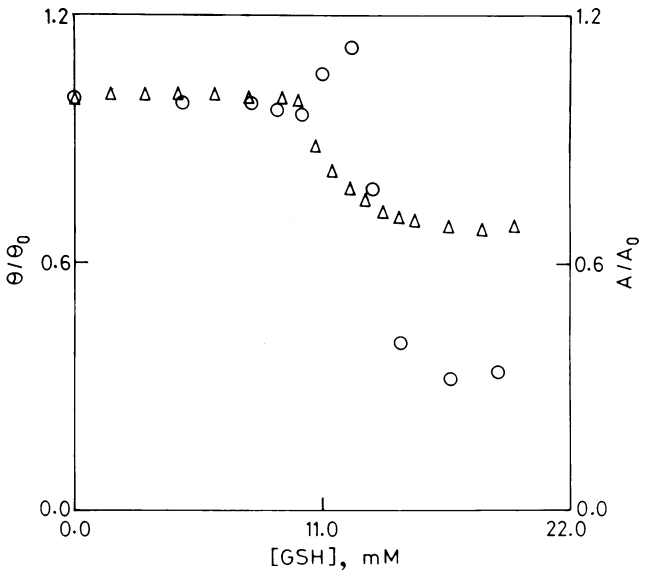

FIG. 4. Titration profiles for the binding of $(CHR)_2Mg^{2+}$ complex to GSH obtained from different spectroscopic techniques in 20 mM Tris–HCl plus 100 mM NaCl buffer, pH 8.0, at 25°: (1) CD, θ/θ_O, at 440 nm as a function of GSH concentration (○); and (2) absorption, A/A_O, at 405 nm as a function of GSH concentration (△). In the $(CHR)_2Mg^{2+}$ complex, concentrations of CHR and $MgCl_2$ were 15.0 μM and 12 mM, respectively. θ is the ellipticity observed after each addition of GSH, and θ_0 is the observed ellipticity in the absence of GSH. Likewise, A and A_0 represent the absorbance after each addition of GSH and in the absence of GSH, respectively.

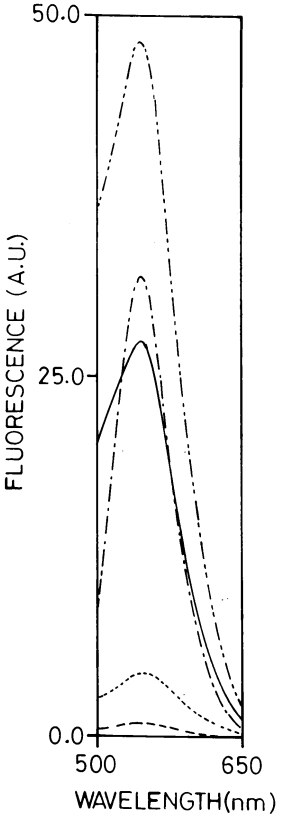

FIG. 5. Fluorescence emission spectra of CHR, $(CHR)_2Mg^{2+}$ complex, and the high complex of GSH under different conditions in 20 mM Tris–HCl plus 100 mM NaCl buffer, pH 8.0, at 25°: (1) CHR (15.0 μM) alone (— · —); (2) $(CHR)_2Mg^{2+}$ complex containing 15.0 μM CHR and 12.0 mM $MgCl_2$ (· · · · · ·); (3) $(CHR)_2Mg^{2+}$ complex in the presence of GSH (18.0 mM, – – – –), i.e. high GSH complex; and (4) high GSH complex in the presence of CT DNA (150 μM, ———) and (750 μM, — · · —).

profiles bring out the differences in the nature of the change observed from absorbance and CD spectroscopy. The second methodology showed the formation of two types of complexes with GSH, when $(CHR)_2Mg^{2+}$ complex bound to it. We did not observe any difference in the nature of the titration profiles in the case of free drug (data not shown). Therefore, we assume that it forms only a single type of complex with GSH.

Henceforth, the complex that was formed at the lower concentration of GSH (12 mM) is referred to as the ***low GSH complex*** of $(CHR)_2Mg^{2+}$ and the one formed at the higher concentration of GSH (≥16 mM), as the ***high GSH complex***, respectively.

The reversible nature of the binding of CHR and $(CHR)_2Mg^{2+}$ complex with GSH was established as follows. A comparison of the reversed-phase HPLC profiles of the drug (or its Mg^{2+} complex) and its equilibrium mixture with GSH showed that the free as well as the GSH-bound CHR eluted at the same place, thereby indicating the reversibility of the interaction and the absence of formation of a covalent complex with GSH (data not shown).

DNA Binding Potential of the GSH-Bound Antibiotic and $(CHR)_2Mg^{2+}$ Complex

Since the antibiotic is established as a DNA-binding inhibitor of replication and transcription, we examined the DNA-binding properties of the GSH-bound CHR in the absence and presence of Mg^{2+}.

Absorption, fluorescence, and CD studies showed that the spectrum of the GSH-bound antibiotic did not change upon the addition of DNA in the absence of Mg^{2+} (data not shown). On the other hand, absorbance, CD, and fluorescence spectra of both low and high GSH complexes underwent a considerable change upon the addition of DNA (Fig. 3 and 5), thereby showing that they bind to DNA. It also indicated that the obligatory requirement of a divalent metal ion for the association of the antibiotic with DNA [9] is maintained for its GSH-bound form. GSH-bound $(CHR)_2Mg^{2+}$ complexes did not bind to poly (dA-dT) as verified by the absence of change in the absorption spectra of the ligands upon the addition of the polynucleotide. This suggests that GC base specificity is not altered upon association with GSH. Experiments with supercoiled plasmid DNA *pARC035* showed the absence of a new band corresponding to relaxed DNA, when the supercoiled DNA was incubated with the high GSH complex of $(CHR)_2Mg^{2+}$ for a period of about 4 hr. This indicates that the DNA remains in the same topological

form. This observation eliminates the possibility of the GSH complexes causing a nick in the DNA strand.

An analysis of spectral changes such as those shown in the figures mentioned above indicates the following general trends. A red shift compared with the unbound ligand, and an increase in the molar extinction value near the 400–440 nm region ensue the binding of the ligand(s) to DNA (Fig. 3a). An increase in the fluorescence emission intensity and a blue shift of the emission peak relative to that of the free ligand are the two features in the fluorescence spectra characterizing the binding of the complexes to DNA (Fig. 5). This is in contrast to the red shift of the fluorescence peak for the $(CHR)_2Mg^{2+}$complex when it binds to DNA [9]. CD spectral changes upon addition of DNA provided further evidence for the binding of high and low GSH complexes with DNA. The most general feature was the increase in the CD band intensity around 440 nm. The resultant spectrum in the presence of DNA was not overlapping with that obtained upon the addition of DNA to the $(CHR)_2Mg^{2+}$ complex in the absence of GSH (Fig. 3b). It indicates that the overall nature of the DNA-bound ligands is different in both cases. Thus, the addition of DNA does not lead to a dissociation of GSH from the $(CHR)_2Mg^{2+}$ complex.

A representative binding isotherm is shown in Fig. 6a. From the binding isotherms, analysis was done to determine the apparent affinity constants, K_{app}, as described under Materials and Methods. The non-cooperative nature of the binding isotherm led us to a Scatchard analysis of the data (shown in Fig. 6b). The relevant binding parameters are summarized in Table 1. The results of the analysis by the two methods were found to be self-consistent within the limits of experimental errors. Since there was no significant deviation of the points in the Scatchard plot from linearity near the abscissa, McGhee–Von Hippel analysis of the binding was not attempted. The single temperature values of the affinity parameters for DNA binding of the different GSH complexes show that the DNA-binding affinity for the drug dimer was relatively higher than for the low and high GSH complexes. The affinity was lowest in the case of the high GSH complex. The stoichiometries were comparable for the binding of all the different ligands to DNA (6–7 bases/drug).

Since the enthalpy–entropy compensation may lead to comparable free energy changes, these parameters were determined to characterize the DNA-binding properties of the two GSH complexes. They were evaluated from the measurement of apparent binding constants at four temperatures. A plot of ln K_{app} against $1/T$ was constructed from which the values of ΔH (from the slope) and ΔS (from the intercept) were determined (Fig. 6c). Then the values of ΔG were calculated from these values (see Materials and Methods). The stoichiometry of binding did not alter with the temperature. The estimated values are summarized in Table 2, and the following features emerge from a scrutiny of this information. Both high and low GSH complexes of $(CHR)_2Mg^{2+}$ bind to DNA via an enthalpy-driven process. On the other hand, past results from our laboratory showed that the $(CHR)_2Mg^{2+}$ complex binds to DNA in an entropy-driven manner [9]. These observations are significant because they demonstrate that the presence of GSH perturbs the association of the $(CHR)_2Mg^{2+}$ complex with DNA and lend support to our previous observation that the addition of DNA does not lead to dissociation of GSH from $(CHR)_2Mg^{2+}$ complex.

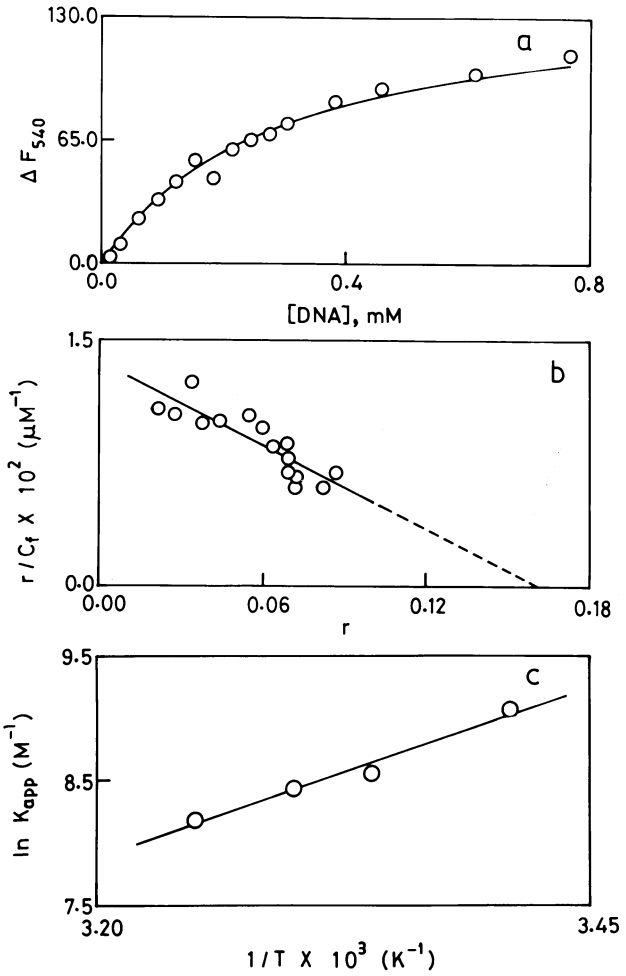

FIG. 6. (a) Binding isotherm (fluorescence emission intensity ΔF_{540} of ligand as a function of DNA concentration) obtained by the curve-fitting method for the interaction of high GSH complex of $(CHR)_2Mg^{2+}$ with DNA in 20 mM Tris–HCl plus 100 mM NaCl buffer, pH 8.0, at 35°. Experimental points (○) are fitted with the theoretical best-fit curve. In the $(CHR)_2Mg^{2+}$ complex, the concentrations of CHR and $MgCl_2$ were 15.3 μM and 12.0 mM, respectively. The high GSH complex contained 18.0 mM GSH. (b) Scatchard plot for the interaction of low GSH complex of $(CHR)_2Mg^{2+}$ with CT DNA in 20 mM Tris–HCl plus 100 mM NaCl buffer, pH 8.0, at 30°. In the $(CHR)_2Mg^{2+}$ complex, the concentrations of CHR and $MgCl_2$ were 15.0 μM and 12.0 mM, respectively; and the low GSH complex contained 12.0 mM GSH. (c) van't Hoff plot for the interaction of high GSH complex of $(CHR)_2Mg^{2+}$ with CT DNA in 20 mM Tris–HCl plus 100 mM NaCl buffer, pH 8.0.

DISCUSSION

The above experimental results show that reduced GSH binds reversibly to the free CHR and $(CHR)_2Mg^{2+}$ com-

TABLE 1. Binding parameters for the interaction of GSH-bound $(CHR)_2Mg^{2+}$ Complex with CT DNA at 20 mM Tris-HCl plus 100 mM NaCl, pH 8.0, at 30°*

Complex type	$K_{app}(\times 10^4\ M^{-1})$†	$K_{app}(\times 10^4\ M^{-1})$‡	n‡
$(CHR)_2\ Mg^{2+}$	2.1	4.3	0.17
Low complex ([GSH] = 12.0 mM)	0.9	1.2	0.15 ± 0.01
High complex ([GSH] = 18.0 mM)	0.5	0.8	0.15 ± 0.01

* $(CHR)_2Mg^{2+}$ complex was prepared by incubating 15 μM CHR with 12 mM $MgCl_2$ for 1 hr. This was followed by the addition of GSH (the concentration is mentioned in the parentheses) and incubation for 30 min. The values were obtained by spectrofluorometric titration as shown in Fig. 5, where separate aliquots of the prepared complex were incubated with increasing concentrations of CT DNA, for 4 hr. Each incubation was done in the dark at 30°. Fluorescence signals (λ_{ex} = 470 nm) of the incubated samples were noted at 540 nm.

† Binding constants were determined using the best-fitted theoretical curve method, as described in Materials and Methods.

‡ Binding constant, K_{app} (M^{-1}), and binding stoichiometry, n (drug molecules bound per nucleotide), were determined using a Scatchard plot as described in Materials and Methods. The value of n is an average of three independent sets of experiments; ± values denote standard error.

plex. The reversible nature of the interaction is the feature that distinguishes it from other antibiotics such as enediynes or bleomycins. These complexes could be formed under *in vivo* conditions also, because the intracellular concentration of GSH lies in the range of 0.5 to 10 mM [12]. The possibility further increases in tumor cells where the GSH level goes up [13, 14]. The moderate salt concentration used in the buffer (100 mM NaCl) eliminates the possibilities of non-specific association involving negatively charged GSH at pH 8.0 in our studies.

There is an important difference between CHR and $(CHR)_2Mg^{2+}$ complex in the nature of the association with GSH. It forms two types of complexes with the drug dimer, $(CHR)_2Mg^{2+}$. The difference in the molecular nature of the GSH-bound complexes of the free drug and the $(CHR)_2Mg^{2+}$ complexes is indicated from their spectroscopic properties such as absorbance and CD, and their DNA-binding properties as well.

The experimental results are discussed as follows: interaction of CHR and its $(CHR)_2Mg^{2+}$ complex with GSH and association of the GSH-bound $(CHR)_2Mg^{2+}$ complexes with CT DNA.

Interaction of Chromomycin A_3 and the $(CHR)_2Mg^{2+}$ Complex with GSH

The binding of the antibiotic and its Mg^{2+} complexes to reduced GSH is characterized by changes in the absorbance and chiro-optical properties of the antibiotic. In general, change in the absorption spectrum of free drug or $(CHR)_2Mg^{2+}$ complex upon binding to GSH could be attributed to an alteration in the local electronic environment of the aglycone chromophore. The presence of negatively charged GSH is a potential source for such perturbation in an electronic environment. The hypochromic effect in the absorption spectra originates from the stacking of the chromophores in the aggregated CHR or $(CHR)_2Mg^{2+}$ complex. A similar trend was also noticed when the antibiotic underwent self-association at a higher concentration (unpublished results). Therefore, it may be suggested that complex formation with GSH leads to self-association of the drug. However, the self-associated forms are different in the case of CHR and $(CHR)_2Mg^{2+}$ complex, as apparent from the non-overlapping nature of the final spectra in the presence of GSH (compare Figs. 2a and 3a). The cooperative nature of the binding profiles (Fig. 4) provides further evidence in support of aggregation of the antibiotic when it binds to GSH.

TABLE 2. Thermodynamic parameters for the interaction of GSH-bound $(CHR)_2Mg^{2+}$ Complex with CT DNA, in 20 mM Tris–HCl plus 100 mM NaCl, pH 8.0*

Complex type	ΔH (kcal/mol)	ΔS (e.u.)	ΔG† (kcal/mol)
$(CHR)_2Mg^{2+}$	8.1†	46.3‡	−5.9
Low complex ([GSH] = 12.0 mM)	−12.6	−23.6	−5.4
High complex ([GSH] = 18.0 mM)	−10.8	−19.1	−5.0

*Complex preparation and titration with CT DNA was done as described in the legend to Table 1 at four different temperatures: 20°, 25°, 30°, and 35°. The thermodynamic parameters were determined by the van't Hoff method, as stated in Materials and Methods. A representative example is shown in Fig. 6c.

†ΔG values were determined at 30°.

‡From Ref. 9.

The CD spectral changes provide more information about the physical process associated with the binding because it originates from the optical asymmetric properties of the aglycone ring in the GSH-bound antibiotic. They show a major difference in the GSH-binding properties of CHR and $(CHR)_2Mg^{2+}$ complex, namely, the formation of a second species at an intermediate GSH concentration (~12 mM) for the $(CHR)_2Mg^{2+}$ complex. In this case, the CD titration profile is multiphasic in nature (Fig. 4). The increase in ellipticity at an intermediate concentration of GSH is a characteristic property in the presence of Mg^{2+}, which induces a certain conformational change of the GSH-bound species. The nature of the CD spectrum at ~12 mM GSH (Fig. 3b) originates from an ordered structure. Such enhanced ellipticity is the feature of a regular structure, permitting a helical flow of charge [26]. Mg^{2+} reduces the electrostatic repulsion between the negatively charged drug and GSH molecules, thereby favoring the formation of an ordered structure. Direct or water-mediated H-bond formation involving different potential loci in the tripeptide and $(CHR)_2Mg^{2+}$ complex might also give rise to such an ordered structure [27].

On the other hand, in the high GSH complex formed at a relatively higher concentration of GSH (≥16 mM), the above ordered structure is perturbed due to ionic contributions from negatively charged GSH and hydrophobic interactions between the chromophores of the antibiotic. It leads to a disordered structure of the chromophores in CHR or its Mg^{2+} complex. Such aggregation would result in a decrease in CD band intensity of the high GSH complex relative to $(CHR)_2Mg^{2+}$ complex (Fig. 3b).

Interaction of the GSH-bound $(CHR)_2Mg^{2+}$ Complexes with CT DNA

DNA-binding properties of the GSH-bound Mg^{2+} complexes of the antibiotic were examined, because DNA is the prime cellular target. The differences between the low and the high complex of GSH as DNA-binding ligands were checked and compared with that for $(CHR)_2Mg^{2+}$ complex in the absence of GSH.

DNA-binding properties of the antibiotic characterized in the absence of GSH are retained even in its presence, e.g. the obligatory requirement of a divalent metal ion and GC base specificity. The possibility of the formation of any covalent interaction between the high and low GSH complex and DNA appears remote, from the absence of any nick in the supercoiled DNA. Similarly, we did not notice any change in the binding when the studies were carried out in a nitrogen atmosphere. It suggests that oxygen does not affect the binding, thereby further reducing the possibility of a covalent interaction via a free radical mechanism, as reported in the case of other antibiotic–GSH interaction [12, 13].

A comparison of the affinity parameters among $(CHR)_2Mg^{2+}$ and its low and high GSH complexes for association with DNA showed that the first one has the highest affinity, binding stoichiometry being comparable for all of them. These results suggest that under *in vivo* conditions, either of the GSH complexes has the potential to bind to DNA. A change in the mode of recognition of DNA by the $(CHR)_2Mg^{2+}$ complex due to its association with GSH is established from the thermodynamic parameters. The effect of GSH upon the DNA-binding properties of the low and high complex of $(CHR)_2Mg^{2+}$ is clearly indicated when we compare the thermodynamic parameters associated with the binding of different ligands to DNA, as shown in Table 2. The presence of GSH changes the entropy-driven interaction of $(CHR)_2Mg^{2+}$ complex with DNA to an enthalpy-driven interaction. The thermodynamic parameters associated with the binding to DNA are not much different among the low and high GSH complexes. In an earlier report, we proposed an alteration of the DNA structure at the binding site of the $(CHR)_2Mg^{2+}$ complex in order to account for the positive enthalpy change [10]. In the absence of any direct evidence, it may be surmised that anionic GSH may be involved in the formation of a noncovalent bond, such as an H-bond, when low and high GSH complexes bind to DNA. It may lead to a favorable enthalpy change, thereby making the interaction enthalpy-driven. The negative change in entropy is another distinctive feature for the association of $(CHR)_2Mg^{2+}$ complex with DNA in the presence of GSH. Insufficient data prevent us from identifying the origin of the above change, which could result from the ordering of the solvent molecules and counterions when the low and high GSH complexes bind to DNA. The negative value of the entropy change for the GSH complexes may, therefore, be attributed to the reorientation of the $(CHR)_2Mg^{2+}$ in the individual complexes prior to binding to DNA. This would lead to a more constrained arrangement of ligand and solvent. In the above processes, the possibility of negatively charged GSH interacting directly with DNA is distant, because it does not bind to DNA at this range of concentration. The differences in the values of the thermodynamic parameters are not significant enough to suggest that the high and low GSH complexes are different DNA-binding ligands. However, the non-overlapping nature of the DNA-bound spectra (absorption and CD) for the GSH complexes of $(CHR)_2Mg^{2+}$ (Fig. 3, a and b) suggest that their DNA-bound forms have different molecular structures.

GSH is a reducing agent that covalently modifies many antibiotics, culminating in damage of DNA by these modified antibiotics, thus enhancing their cytotoxicity. From our results, such a possibility in the case of CHR appears very remote. The reason for the high cytotoxicity of the aureolic acid group of antibiotics may be ascribed to their interaction at some other cellular site, e.g. a recent report has shown that a structurally related drug, mithramycin, binds to the cytoskeletal protein spectrin [28].

S. C. wishes to thank Professor (Dr.) B. Sinha, Director of the S.I.N.P., for his permission to allow her to work in the Biophysics Division. We also thank Professor S. K. Ghosh of the Crystallography & Molecular Biology Division of our Institute for making available a Jasco J-720 spectropolarimeter.

REFERENCES

1. Gause GF, Olivomycin, chromomycin and mithramycin. In: *Antibiotics III, Mechanism of Action of Antimicrobial Antitumor Agents* (Eds. Corcoran JW and Hahn FE), Vol. II, pp. 197–202. Springer, Berlin, 1975.
2. Chabner BA, Allegra CJ, Curt GA and Calabresi P, Antineoplastic agents. In: *Goodman & Gilman's The Pharmacological Basis of Therapeutics* (Eds. Hardman JG, Limbird LE, Molinoff PB, Ruddon RW and Gilman AG), 9th Edn, pp. 1233–1287. McGraw-Hill, New York, 1996.
3. Sastry M, Fiala R and Patel DJ, Solution structure of mithramycin dimers bound to partially overlapping sites on DNA. *J Mol Biol* **251:** 674–689, 1995.
4. Keniry MA, Banville DL, Simmonds PM and Shafer RH, Nuclear magnetic resonance comparison of the binding sites of mithramycin and chromomycin on the self-complementary oligonucleotide $d(ACCCGGGT)_2$. *J Mol Biol* **231:** 753–767, 1993.
5. van Dyke MW and Dervan PB, Chromomycin, mithramycin and olivomycin binding sites on heterogeneous deoxyribonu-

cleic acid. Footprinting with (methidiumpropyl-EDTA)iron (II). *Biochemistry* **22:** 2373–2377, 1983.
6. Stankus A, Goodisman J and Dabrowiak JC, Quantitative footprinting analysis of the chromomycin A_3–DNA interaction. *Biochemistry* **31:** 9310–9318, 1992.
7. Goldberg IH and Friedman PA, Antibiotics and nucleic acids. *Annu Rev Biochem* **40:** 775–810, 1971.
8. Aich P, Sen R and Dasgupta D, Interaction between antitumor antibiotic chromomycin A_3 and Mg^{2+}. I. Evidence for the formation of two types of chromomycin A_3–Mg^{2+} Complexes. *Chem Biol Interact* **83:** 23–33, 1992.
9. Aich P, Sen R and Dasgupta D, Role of magnesium ion in the interaction between chromomycin A_3 and DNA: Binding of chromomycin A_3–Mg^{2+} complexes with DNA. *Biochemistry* **31:** 2988–2997,1992.
10. Majee S, Sen R, Guha S, Bhattacharyya D and Dasgupta D, Differential interactions of the Mg^{2+} complexes of chromomycin A_3 and mithramycin with poly(dG-dC) · poly(dC-dG) and poly(dG) · poly(dC). *Biochemistry* **36:** 2291–2299, 1997.
11. Gilbert HF, Thiol/disulfide exchange equilibria and disulfide bond stability. *Methods Enzymol* **251** (Part A)**:** 8–28, 1995.
12. Meister A and Anderson ME, Glutathione. *Annu Rev Biochem* **52:** 711–760, 1983.
13. Cook AJ and Mitchell JB, Measurement of thiols in cell population from tumor and normal tissue. *Methods Enzymol* **251** (Part A)**:** 203–212, 1995.
14. Hormas RA, Andrews PA, Murphy MP and Burns CP, Glutathione depletion reverses cisplatin resistance in murine L1210 leukemia cells. *Cancer Lett* **34:** 913, 1987.
15. Gao X, Stassinopoulos A, Rice JR and Goldberg IH, Structural basis for the sequence-specific DNA strand cleavage by the Enediyne neocarzinostatin chromophore. Structure of the post-activated chromophore–DNA complex. *Biochemistry* **34:** 40–49, 1995.
16. Myers AG, Cohen SB and Kwon BM. A study of the reaction of calicheamicin γ1 with glutathione in the presence of double-stranded DNA. *J Am Chem Soc* **116:** 1255–1271, 1994.
17. Glover D, Fox KR, Weiler C, Kligerman MM, Turrisi A and Glock JH, Clinical treats of WR-2721 prior to alkylating agent chemotherapy and radiotherapy. *Pharmacol Ther* **39:** 3–7, 1988.
18. Révész L and Modig H, Cysteamine-induced increase of cellular glutathione-level: A new hypothesis of the radioprotective mechanism. *Nature* **207:** 430–431, 1965.
19. Nayak R, Sirsi M and Podder SK, Role of magnesium ions on the interaction between chromomycin A_3 and deoxyribonucleic acid. *FEBS Lett* **30:** 157–162, 1973.
20. Anderson ME, Determination of glutathione and glutathione disulfide in biological samples. *Methods Enzymol* **113** (Part A)**:** 548–555, 1985.
21. Sambrook J, Fritsch EF and Maniatis T, Plasmid vectors. In: *Molecular Cloning* (Ed. Nolan C), Vol. 1, 2nd Edn, pp. 1.33–1.39. Cold Spring Harbor Laboratory Press, Cold Spring Harbor, NY, 1989.
22. Cobuzzi RJ, Kotsopoulos SK, Otani T and Beerman TA, Effects of the enediyne C-1027 on intracellular DNA targets. Biochemistry **34:** 583–592, 1995.
23. Wang JL and Edelman GM, Fluorescence probe for conformational states of proteins. IV. The pepsinogen-pepsin conversion. J Biol Chem **246:** 1185–1191, 1971.
24. Härd T, Hsu V, Sayre MH, Geiduschek EP, Appelt K and Kearns DR, Fluorescence studies of a single tyrosine in a type II DNA binding protein. *Biochemistry* **28:** 396–406, 1989.
25. Castellan GW, Chemical reactions and the entropy of the universe. In: *Physical Chemistry* (Indian Student edition), 3rd Ed, pp. 799–815. Addison-Wesley, Reading, MA, U.S.A. and Narosa Publishing House, New Delhi, 1989.
26. Cantor CR and Schimmel PR, Other optical techniques. In: *Biophysical Chemistry*, Part III, pp. 409-480. Freeman, San Francisco, 1980.
27. Reinemer P, Dirr HW and Huber R, X-Ray structure methods for glutathione binding. *Methods Enzymol* **251** (Part A)**:** 243–254, 1995.
28. Majee S and Chakrabarti A, A DNA-binding antitumor antibiotic binds to spectrin. *Biochem Biophys Res Commun* **212:** 428–432, 1995.